Supporting Information

A Ring of Grids: A Giant Spin-Crossover Cluster

Takuya Shiga,*[a] Minami Tachibana,[a] Hajime Sagayama,[b] Reiji Kumai,[b]

Graham N. Newton,[c] Hiroki Oshio[a,d] and Masayuki Nihei[a]

a. Graduate School of Pure and Applied Sciences, University of Tsukuba, Tennodai 1-1-1, Tsukuba, Ibaraki 305-8571, Japan.
b. Photon Factory and Condensed Matter Research Center, Institute of Materials Structure Science, High Energy Accelerator Research Organization (KEK), Oho 1-1, Tsukuba, Ibaraki 305-0801, Japan.
c. GSK Carbon Neutral Laboratories for Sustainable Chemistry, University of Nottingham, Nottingham, NG7 2TU, U.K.
d. State Key Laboratory of Fine Chemicals, Dalian University of Technology, 2 Linggong Rd., 116024 Dalian, China

Corresponding author
Dr. Takuya Shiga
Graduate School of Pure and Applied Sciences,
University of Tsukuba
Tennodai 1-1-1, Tsukuba, Ibaraki 305-8571 (Japan)
TEL: (+81)29-852-4426
FAX: (+81)29-852-4426
E-mail: shiga@chem.tsukuba.ac.jp

Table of Contents

Experimental Procedures

Description of chemicals

All solvents and chemicals were reagent grade, purchased commercially, and used without further purification unless otherwise noted. The precursor of multidentate ligand, 6-(3,5-dimethylpyrazol-1-yl)-2-pyridinecarboxyaldehyde, was prepared following the published syntheses.[1]

Synthetic procedures

Synthesis of 2-hydroxy-1-[6-(3,5-dimethyl-1*H*-pyrazol-1-yl)pyrid-2-yl]-2-(2-pyridinyl)ethanone

To a mixture solution of 6-(3,5-dimethylpyrazol-1-yl)-2-pyridinecarboxyaldehyde (904 mg, 4.50 mmol) and 2-pyridinecarboxaldehyde (2.13 mL, 22.5 mmol) in 30 mL ethanol was added an aqueous solution of potassium cyanide (293 mg, 4.51 mmol). The resulting solution was stirred at room temperature for 15 mins. A yellow precipitate (2.98 g) was collected by filtration. This precipitate is mixture of 2-hydroxy-1-[6-(3,5-dimethyl-1*H*-pyrazol-1-yl)pyrid-2-yl]-2-(2-pyridinyl)ethanone, 2-hydroxy-1,2-di-2-pyridinylethanone, and 1,2-bis[6-(3,5-dimethyl-1*H*-pyrazol-1-yl)pyrid-2-yl]-2-hydroxyethanone, which are confirmed by NMR and MS. The crude mixture was used for the following synthetic procedure without any purification.

Synthesis of 2-hydroxy-1-[6-(3,5-dimethyl-1*H*-pyrazol-1-yl)pyrid-2-yl]-2-(2-pyridinyl)glyoxal

The crude yellow solid (2.98 g) was dissolved in concentrated nitric acid (13 mL). After the evolution of nitrogen dioxide gas had subsided, the solution was neutralized (pH = 6) with a saturated aqueous solution of potassium hydroxide. A precipitated brown solid was collected by filtration and purified by column chromatography on silica gel (eluting with ethyl acetate/*n*-hexane = 1:1) to give 2-hydroxy-1-[6-(3,5-dimethyl-1*H*-pyrazol-1-yl)pyrid-2-yl]-2-(2-pyridinyl)glyoxal (548 mg, 1.79 mmol) as a pale yellow solid. Yield: 40 %. R_f=0.58 (AcOEt/n-Hexane 1:1); ^{1}H NMR (400 MHz, $CDCl_3$): δ=8.61-8.59 (m, 1H), 8.19-8.16 (m, 2H), 8.04 (d, *J*=7.6 Hz, 1H), 8.00 (d, *J*=8.0 Hz, 1H), 7.51-7.48 (m, 1H), 7.29 (dd, *J*=7.6Hz, *J*=8.0Hz, 1H), 5.85 (s, 1H), 2.23 (s, 3H), 2.06 ppm (s, 3H); IR (KBr): **Error!** = 3101(w), 2930(w), 1713(s), 1695(s), 1582(s), 1483(s), 1456(s), 1441(m), 1387(s), 1368(m), 1285(m), 1223(s), 1053(w), 993(m), 974(m), 905(m), 799(m), 758(s), 747(m), 675(m), 650(m), 615(m) cm^{-1}; MS (ESI): *m*/*z* calcd for $C_{17}H_{14}N_4O_2$+Na$^+$: 329.31 [*M*+Na]$^+$; found: 329.10; elemental analysis calcd (%) for $C_{17}H_{14}N_4O_2$: C 66.66, H 4.61, N 18.29; found: C 66.27, H 4.64, N 18.02.

Synthesis of 2-phenyl-4,5-bis{6-(3,5-dimethyl pyrazol-1-yl)pyrid-2-yl]-1*H*-imidazol (HL)

2-Hydroxy-1-[6-(3,5-dimethyl-1*H*-pyrazol-1-yl)pyrid-2-yl]-2-(2-pyridinyl)glyoxal (545 mg, 1.78 mmol), benzaldehyde (181 μL, 1.78 mmol) and ammonium acetate (1.37 g, 17.8 mmol) were dissolved in acetic acid (21 mL) and irradiated by microwave (180 ^{o}C, 200 W) for 5 mins. To the resulting mixture was added cold water (20 mL) and the mixture was neutralized by addition of saturated sodium hydroxide solution. The resulting precipitate was extracted into dichloromethane, and the organic phase was dried over anhydrous magnesium sulphate. The solvent was removed in vacuo, affording pale yellow powder of HL (636 mg, 1.61 mmol, 91 % yield). ^{1}H NMR (400 MHz, $CDCl_3$): δ=10.81 (s, 1H), 8.72-8.65 (m, 2H), 8.58-8.57 (m, 2H), 8.20-7.95 (m, 6H), 7.94-7.90 (t, 1H), 7.86-7.53 (m, 6H), 7.52-7.48 (m, 4H), 7.45-7.42 (m, 2H), 7.30-7.13 (m, 2H), 6.09 (s, 1H), 5.95 (s, 1H), 2.77 (s, 3H), 2.34 (s, 3H), 2.33 (s, 3H), 2.32 ppm (s, 3H); IR (KBr): **Error!**= 3063(w), 2924(w), 1591(s), 1489(s), 1466(s), 1379(m), 1362(m), 1294(w), 1146(w), 1088(w), 1028(w), 980(w), 812(m), 791(m), 710(m), 692(m) cm^{-1}; MS (ESI): *m*/*z* calcd for $C_{24}H_{20}N_6$+H$^+$: 393.17 [*M*+H]$^+$; found: 393.18; elemental analysis calcd (%) for $C_{24}H_{21}N_6O_{0.5}$: C 71.80, H 5.27, N 20.93; found: C 71.54, H 5.34, N 20.73.

Synthesis of $[Fe(L)_2](BF_4)_2 \cdot 1.5H_2O$ (1)

To a solution of $Fe(BF_4)_2$ $6H_2O$ (17.1 mg, 0.051 mmol) in acetonitrile (5.0 mL) was added a solution of HL (39.4 mg, 0.10 mmol) in acetonitrile (5.0 mL). The resulting red solution was stirred for one hour. After filtration, ethyl acetate was allowed to diffuse into the solution, resulting in the formation of yellow plates of $[Fe^{II}(HL)_2](BF_4)_2$•AcOEt•$2H_2O$. Yellow crystals were collected by filtration and air-dried (28.4 mg, 0.028 mmol, 55 % yield). IR (KBr): **Error!**=3424(br), 1609(m), 1560(m), 1490(s), 1477(s), 1420(m), 1084(s), 791(w), 723(w) cm^{-1}; elemental analysis calcd (%) for $C_{48}H_{43}B_4F_8FeN_{12}O_{1.5}$ ($[Fe^{II}(HL)_2](BF_4)_2$•1.5H_2O): C 55.36, H 4.16, N 16.14; found: C 55.31, H 4.11, N 16.04. TG data: -3.00 % at 51.5 ^{o}C. Calcd. for loss of 1.5 H_2O: 2.60 %.

Synthesis of $[Fe_{20}(L)_{24}](BF_4)_{16} \cdot 35H_2O$ (2)

A solution of $Fe(BF_4)_2$ $6H_2O$ (17.0 mg, 0.050 mmol) in DMF (3.0 mL) was added a solution of HL (23.7 mg, 0.060 mmol) and DBU (8.97 μL, 0.060 mmol) in DMF (2.0 mL). The resulting dark-red solution was stirred for two hours. After filtration, ethyl acetate was allowed to diffuse into the solution, resulting in the formation of dark red plates of $[Fe^{II}_{20}(L)_{24}](BF_4)_{16}$•n(solv.). Red crystals were collected by filtration (8.80 mg, 0.00087 mmol, 27 % yield). IR (KBr): $\tilde{\nu}$=3414(br), 1603(s), 1560(s), 1474(s), 1420(m), 1364(m), 1084(s), 787(w), 725(w) cm^{-1}; elemental analysis calcd (%) for $C_{576}H_{526}B_{16}F_{64}Fe_{20}N_{144}O_{35}$ ($[Fe^{II}_{20}(L)_{24}](BF_4)_{16}$•35$H_2O$): C 55.21, H 4.23, N 16.10; found: C 55.29, H 3.98, N 15.83. Single crystals for structural analysis were obtained by using hexyl acetate instead of ethyl acetate. Note that red plates obtained from DMF/AcOEt diffusion have poor crystallinity. However, the following crystal parameters were determined from diffraction data. Crystal parameters: *a* = 18.183(9) Å, *b* = 37.06(2) Å, *c* = 61.49(3) Å, α = 74.541(8) deg, β = 88.073(6) deg, γ = 87.349(5) deg, *V* = 39885(35) Å^3. The yield of red crystals obtained from DMF/AcOHx diffusion is slightly low, therefore physical measurements for the crystals obtained from DMF/AcOEt diffusion were performed. TG data: -4.28 % at 50.0 ^{o}C. Calcd. for loss of 35 H_2O: 5.03 %.

Experimental Details

X-ray crystallography

Single crystal X-ray diffraction measurements were conducted on a Bruker Smart APEX II ULTRA CCD diffractometer using Mo-K_α radiation (λ = 0.71073 Å, 50 kV, 24 mA) with a graphite monochromator for **1** at 300 K and **2**. The synchrotron X-ray measurements for **1** at 20 K and light excited state of **1** were conducted using a diffractometer installed at BL-8A at the Photon Factory, KEK, Tsukuba. Single crystals of **1** and **2** were mounted on a glass rod or micromount, and intensity data were collected at 20 K, 300 K, 20 K (after irradiation 532 nm) for **1**, and at 100 K for **2**. See Table S1 for all parameters. The structures were solved by using direct methods (SHELXS-97) and refined by using full-matrix least-square calculations on F^2 using (SHELXL-2016/6) included in the SHELX-TL program package.[2] All data sets were treated with the SQUEEZE program from the PLATON suite to remove highly disordered solvent molecules from the calculations.[3] In the crystallographic analysis of **1**, electrons in the void space were estimated to 68 e^- per $[Fe(HL)_2](BF_4)_2$ molecule. This contribution was assigned to one ethyl acetate (48 e^-) and two water molecules (10 e^- x 2). In **2**, an electron count of 5810 e^- was obtained for 17503 $Å^3$ volume. The electron density must correspond to BF_4^- anions, DMF, AcOHx, and water molecules. An accurate amount of the solvent molecules cannot be determined based on this crystallographic data.

Magnetic measurements

Susceptibility data were collected under an applied magnetic field of 500 Oe using a Quantum Design MPMS-5S SQUID magnetometer. The temperature dependence was measured at 3.0 K increments in settle mode. The scan rate of the temperature was fixed to 10.0 K min^{-1} above 10 K, and at 2.0 K min^{-1} below 10 K, and each measurement was performed 30 sec after the temperature had stabilized. Magnetic data were corrected for the diamagnetism of the sample holder and of the sample using Pascal's constants. In the light irradiation experiments, a small amount of sample was used to maximize the light conversion ratio. The sample was irradiated at 5 K by a DPSS laser (532 nm with 10 mW cm^2, Opto Tech 532.200.KE.01 and 808 nm with 10 mW cm^2, Intelite I808-120G-CAP) through an optical fibre (Newport F-MBD; 3 m length, 1.0 mm core size, 1. 4mm diameter). During irradiation, the magnetic moment was recorded at regular time intervals until saturation, after which point the light irradiation was stopped. The temperature dependence of magnetic susceptibility after light irradiation was measured using an applied magnetic field of 500 Oe and a scan rate of 0.1 K min^{-1} in sweep mode.

Mössbauer spectra

Mössbauer experiments were carried out using a ^{57}Co/Rh source in a constant-acceleration transmission spectrometer (Topologic Systems) equipped with an Iwatani HE05/CW404 cryostat. The spectrometer was calibrated using standard α-Fe foil.

Structure Analyses (Additional Descriptions)

Complex 1

As described in the main text, complex **1** forms the 1D chain structure through NH···N interactions between imidazole and pyridine moieties. The interatomic distances of two N atoms through the hydrogen bond are 2.877 Å and 2.914 Å at 20 K and 300 K, and 2.878 Å in the light excited state, respectively. These small changes of intermolecular interactions may be originating from the thermal expansion of the cell, and there is no relationship with the spin state of the iron ions. In the case of light excited state, coordination bond lengths and angles are close to the values at the high spin state, while the cell parameters and volumes are almost unchanged from the values at the low spin state.

Complex 2

In **2**, there are four [2x2] grid moieties. Each grid is stabilized by π-π stacking interactions between adjacent ligands (pyridine-phenyl-pyridine stacking). **2** has two unique mononuclear moieties (type C), one of which showed no SCO down to 1.8 K. The mononuclear moieties linked the grid moieties, forming the giant ring molecule. The phenyl rings of the mononuclear unit interact with phenyl rings of the grid moieties through CH-π interactions. These intramolecular interactions may inhibit the structural changes from the HS to the LS state.

Molecular structure of 1

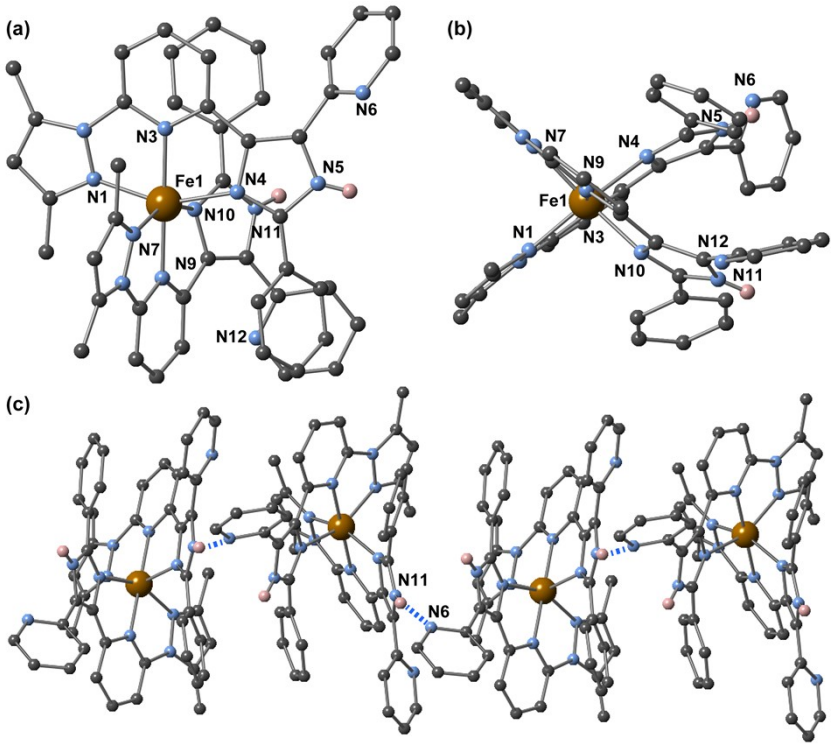

Figure S1. Molecular structure of **1**. (a) Top view, (b) side view, (c) one-dimensional network. Colour code: C, gray; N, light blue; Fe(II), brown; H, pink.

Mössbauer spectra for 1

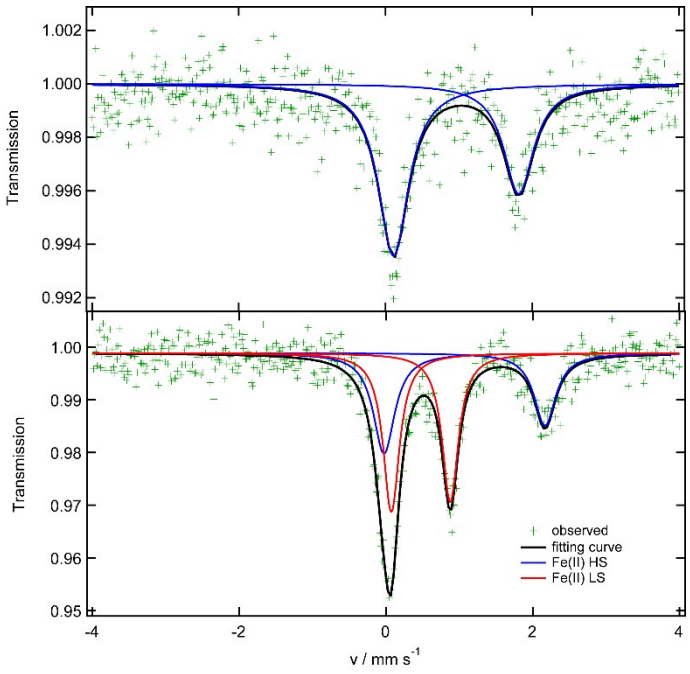

Figure S2. Mossbauer spectra of **1** at 300 K (top) and 50 K (bottom).

Magnetic properties for 1 and 2

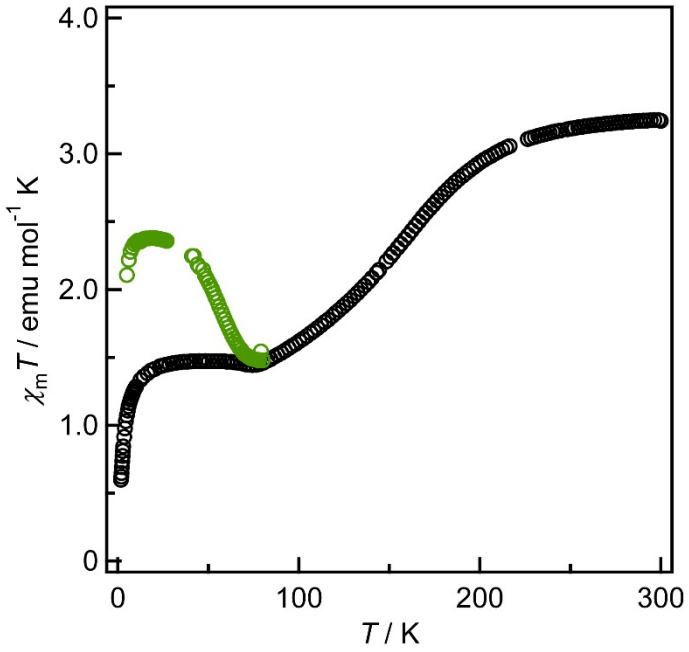

Figure S3. Plots of $\chi_m T$ versus T for **1**. The $\chi_m T$ values in the LIESST state for **1** are shown in green.

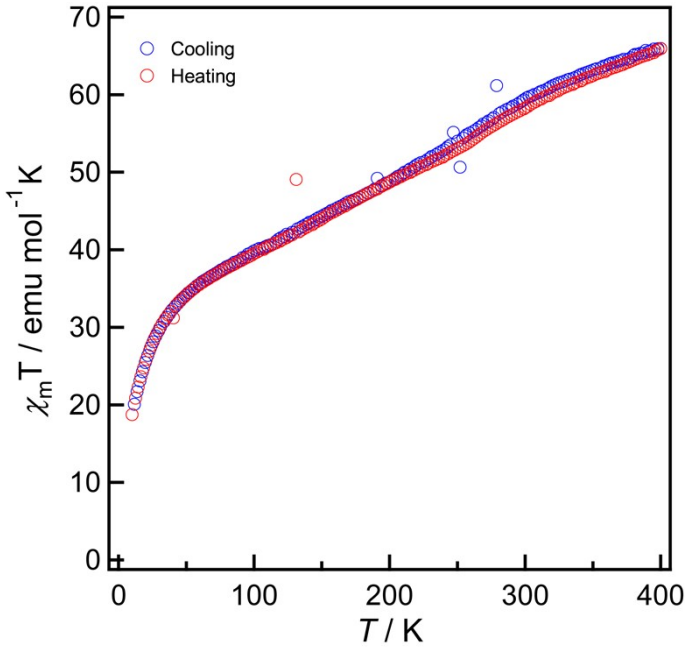

Figure S4. Plots of $\chi_m T$ versus T for a dried sample of **2**.

Schematic representation of structure for 2

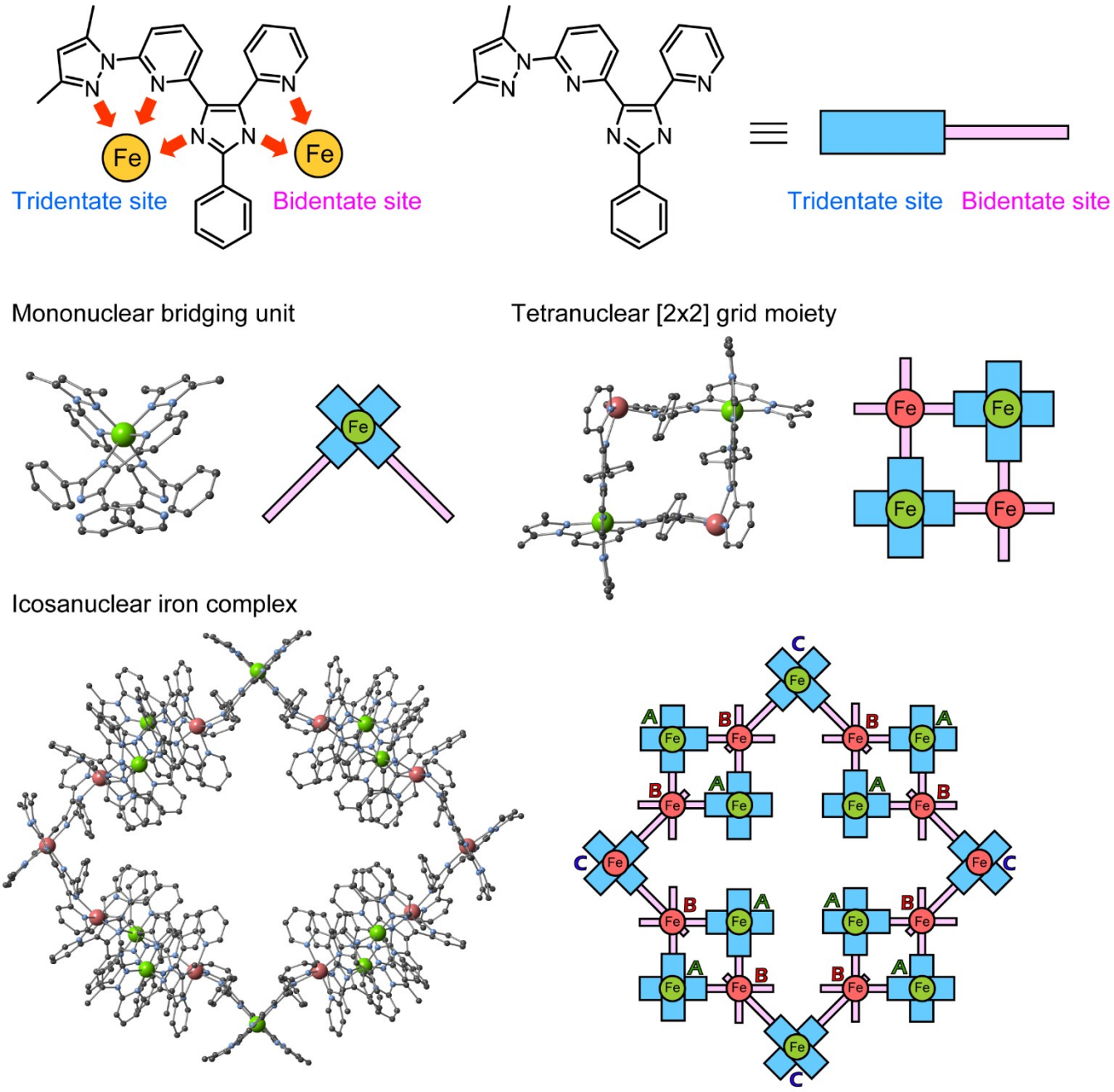

Figure S5. Schematic drawing of structure for **2**.

Mössbauer spectra for 2

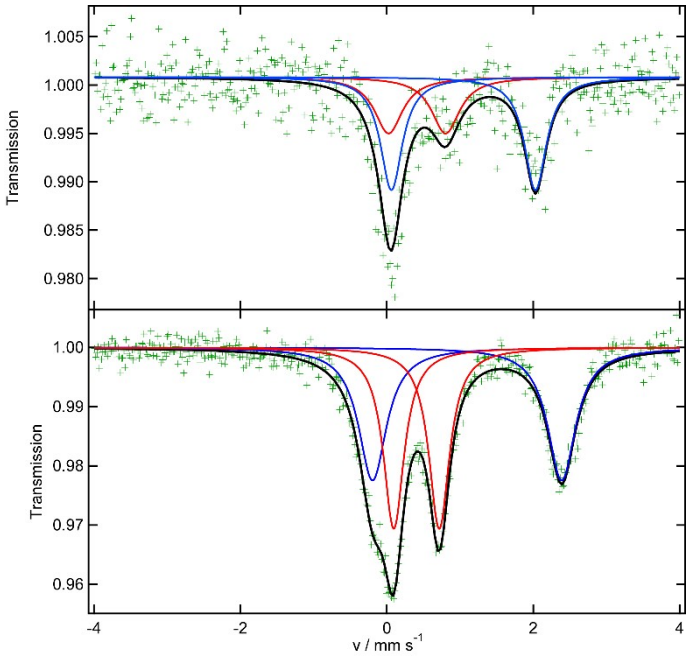

Figure S6. Mossbauer spectra of **2** at 300 K (top) and 20 K (bottom).

Thermogravimetric data for 1 and 2

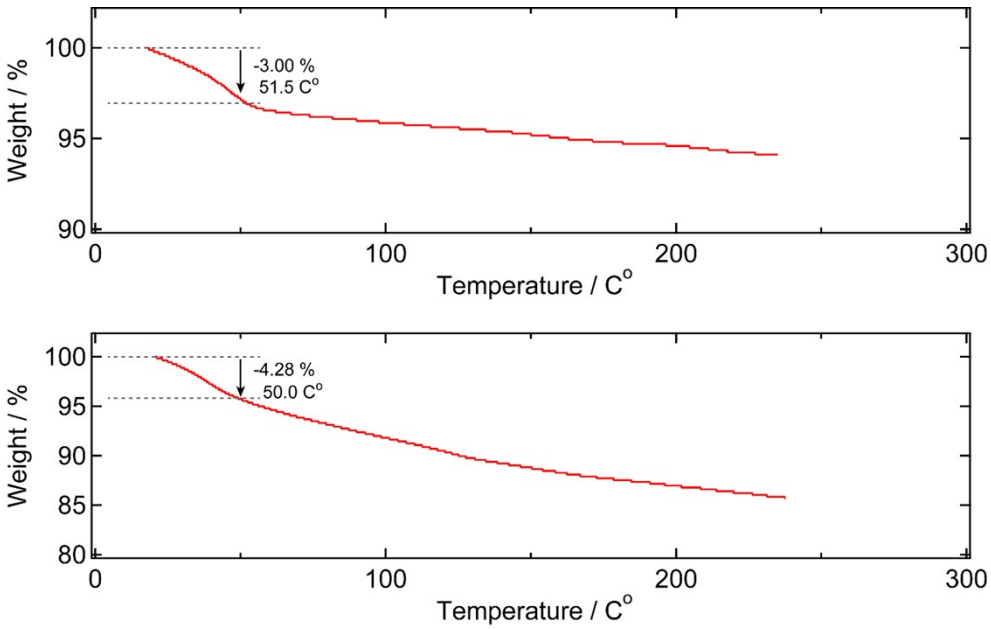

Figure S7. TG data of **1** (top) and **2** (bottom).

Crystallographic data

Table S1. Crystallographic parameters.

	Comp.1 20 K	Comp.1 green	Comp.1 300 K	Comp. 2 100 K
Formula	$C_{48}H_{40}B_2F_8FeN_{12}$	$C_{48}H_{40}B_2F_8FeN_{12}$	$C_{48}H_{40}B_2F_8FeN_{12}$	$C_{582}H_{468}B_4F_{16}Fe_{20}N_{146}O_2$
Fw	1014.39	1014.39	1014.39	11003.24
Crystal system	Monoclinic	Monoclinic	Monoclinic	Triclinic
Space group	$P2_1/c$	$P2_1/c$	$P2_1/c$	P**Error!**
a [Å]	13.1562(6)	13.1659(9)	13.262(6)	18.097(4)
b [Å]	25.4851(10)	25.8307(14)	26.316(13)	36.464(9)
c [Å]	14.9807(7)	15.1275(10)	15.453(8)	62.104(15)
α [°]	90	90	90	73.262(2)
β [°]	104.0270(10)	103.183(2)	103.455(6)	88.260(2)
γ [°]	90	90	90	87.385(2)
V [Å^3]	4873.1(4)	5009.0(5)	5245(4)	39199(16)
Z	4	4	4	2
F(000)	2080	2080	2080	11364
λ [Å]	1.000	1.000	0.71073	0.71073
T [K]	20(2)	20(2)	300(2)	100(2)
ρ_{calcd} [Mg m^{-3}]	1.383	1.345	1.285	0.932
μ [mm^{-1}]	0.388	0.378	0.361	0.411
θ range [° min-max]	2.245 to 37.042	2.219 to 37.041	1.548 to 27.499	1.019 to 25.500
No. of data collected	20187	20727	27569	396427
No. of unique data	8434	8446	11790	145385
R(int)	0.1042	0.1687	0.0827	0.1635
No. of variable parameters	664	644	644	6759
No. of obsd. Refl.	8434	8446	11790	145385
R obsd., $I > 2\sigma(I)$	0.0918	0.1002	0.1529	0.1186
*R*w obsd., $I > 2\sigma(I)$	0.2289	0.2525	0.4327	0.3262
R obsd., all	0.1499	0.2126	0.2307	0.2459
*R*w obsd., all	0.2532	0.2881	0.4770	0.3970
Goodness-of-fit on F^2	0.947	0.854	1.507	1.034
$(\Delta/\rho)_{max,min}$ [e A^{-3}]	0.624 and -0.663	0.690 and -0.536	1.016 and -0.798	0.854 and -0.857

Table S2. The average coordination bond lengths and Σ values of complex **2**.

		Average coordination bond lengths	Σ values / degree	Assignment	Type
Mononuclear units	Fe1	1.949	82.1	LS	C
	Fe2	2.162	149.8	HS	C
	Fe3	1.955	82.8	LS	C
	Fe4	2.149	148.1	HS	C
Grid unit	Fe5	2.171	109.8	HS	B
	Fe6	1.966	85.8	LS	A
	Fe7	2.190	101.7	HS	B
	Fe8	1.957	89.0	LS	A
	Fe9	2.175	94.4	HS	B
	Fe10	1.946	84.0	LS	A
	Fe11	2.178	110.9	HS	B
	Fe12	1.951	87.4	LS	A
	Fe13	2.169	98.1	HS	B
	Fe14	1.957	84.3	LS	A
	Fe15	2.185	97.2	HS	B
	Fe16	1.934	77.7	LS	A
	Fe17	2.169	97.3	HS	B
	Fe18	1.963	80.6	LS	A
	Fe19	2.172	99.2	HS	B
	Fe20	1.956	91.7	LS	A

HS = High Spin, LS = Low Spin

Table S3. The average coordination bond lengths and Σ values of complex **1**.

		Average coordination bond lengths	Σ values / degree	Assignment
Mononuclear complex	20 K	2.077	134.2	A mixture of LS and HS
	Green	2.151	148.7	HS
	300 K	2.172	148.7	HS

Mössbauer data

Table S4. Mössbauer parameters.

		δ_{IS} / mm s^{-1}	ΔE_Q / mm s^{-1}	Area / %	FWHM
Comp. 1 (300 K)	Fe^{II} HS	0.96	1.71	100	0.50
Comp. 1 (50 K)	Fe^{II} LS	0.47	0.80	57	0.27
	Fe^{II} HS	1.07	2.19	43	0.36
Comp. 2 (300 K)	Fe^{II} LS	0.41	0.78	39	0.47
	Fe^{II} HS	1.05	1.97	61	0.36
Comp. 2 (20 K)	Fe^{II} LS	0.41	1.09	50	0.42
	Fe^{II} HS	1.09	2.58	50	0.38

HS = High Spin, LS = Low Spin, FWHM = Full Width at Half Maximum

References

[1] T. Matsumoto, G. N. Newton, T. Shiga, S. Hayami, Y. Matsui, H. Okamoto, R. Kumai, Y. Murakami, H. Oshio, *Nat. Commun.* **2014**, *5*, 3865.

[2] a) A. Altomare, M.C. Burla, M. Camalli, G.L. Cascarano, C. Giacovazzo, A. Guagliardi, A.G.G. Moliterni, G. Polidori, R.J. Spagna, *Appl. Cryst.*, **1999**, *32*, 115-119; b) G.M. Sheldrick, *Acta Cryst.*, **2015**, A71, 3-85; c) G.M. Sheldrick, *Acta Cryst.*, **2015**, *C71*, 3-8; d) G.M. Sheldrick, *Acta Crystallogr., Sect. A: Found. Crystallogr.*, **2008**, *64*, 112-122.

[3] A.L. Spek, PLATON (2002). A Multipurpose Crystallographic Tool. Utrecht University, The Netherlands. (http://www.cryst.chem.uu.nl/platon.)